Hyperfine Interactions 129 (2000) 119–129

High-resolution measurements of low-energy conversion electrons

B. Roussière [a], J. Genevey [b], A. Gizon [b], D. Hojman [a,*], F. Ibrahim [b], P. Kilcher [a], A. Knipper [c], F. Le Blanc [a], G. Marguier [d], J. Obert [a], J. Oms [a], J.C. Putaux [a], C. Richard-Serre [e,f], J. Sauvage [a], A. Wojtasiewicz [a,**], D. Forkel-Wirth [f], J. Lettry [f] and the ISOLDE Collaboration

[a] *Institut de Physique Nucléaire, CNRS-IN2P3/Université Paris XI, F-91406 Orsay Cedex, France*
[b] *Institut des Sciences Nucléaires, CNRS-IN2P3/Université Joseph Fourier, F-38026 Grenoble Cedex, France*
[c] *Institut de Recherches Subatomiques, CNRS-IN2P3/Université Louis Pasteur, F-67037 Strasbourg Cedex 2, France*
[d] *Institut de Physique Nucléaire, CNRS-IN2P3/Université Lyon I, F-69622 Villeurbanne Cedex, France*
[e] *IN2P3, Paris, France*
[f] *ISOLDE/CERN, CH-1211 Geneva 23, Switzerland*

High-resolution measurements of low-energy conversion electrons have been performed in odd and odd–odd nuclei with masses around $A = 182$. The experimental setup, a magnetic spectrograph coupled to a specific tape transport system, is described. Three experiments have been performed and the main results are presented.

1. Introduction

Internal conversion electron measurements bring decisive information in the study of transitional heavy nuclei. Spins and parities are needed to establish the nuclear structure of a given nucleus. This knowledge which is extracted from multipolarities of transitions connecting excited levels can be deduced from precise conversion electron energy and intensity measurements. Moreover, for very low-energy transitions ($E \leqslant 50$ keV) occurring frequently in deformed odd or doubly-odd nuclei, conversion coefficients are very high and it is often impossible to detect them in γ-spectroscopy measurements. In such cases, the only means to point out the transitions is through their conversion lines. Obviously, measurements with high energy resolution are needed to separate the L-conversion lines and even the M ones in order to determine unambiguously the transition multipolarities from the $L_1/L_2/L_3/\ldots$ intensity ratios. Furthermore, the absolute transition probability between nuclear states depends on both the transition multipolarity and the wave functions of the states linked by the transitions. So the transition probabilities deduced from multipolarity measure-

* Permanent address: CNEA, TANDAR, Buenos Aires, Argentina.
** Permanent address: Warsaw University, Warsaw, Poland.

ments provide a powerful means of investigating in more detail the structure of nuclear states.

In this paper, we present several measurements of low-energy internal conversion electrons performed with high energy resolution in some N = 105 odd or odd–odd nuclei. In $^{183}_{78}Pt_{105}$ and $^{181}_{76}Os_{105}$, the purpose of the experiment was to search for the M3 transitions connecting the $\nu\frac{7}{2}[5\,1\,4]$ isomeric state to the $\nu\frac{1}{2}[5\,2\,1]$ ground state and determine their transition probability (B(M3)). In $^{184}_{79}Au_{105}$, these neutron configurations both coupled to the $\pi h_{9/2}$ proton have been proposed to describe the isomeric and ground states [1,2] but the B(M3) transition probability has been found thirty times higher than the value obtained for the $\nu\frac{1}{2}[5\,2\,1] \rightarrow \nu\frac{7}{2}[5\,1\,4]$ transition in $^{179}_{74}W_{105}$ [3]. Comparing the B(M3) values in $^{179}_{74}W_{105}$, $^{181}_{76}Os_{105}$, $^{183}_{78}Pt_{105}$ and $^{184}_{79}Au_{105}$ should allow us to confirm or invalidate the neutron configurations proposed for ^{184m,g}Au and to determine to what extent the B(M3) difference between ^{184}Au and ^{179}W is significant.

In ^{182}Ir, the aim of the experiment was to determine the multipolarity of the low-energy transitions in order to assign spin and parity values to the excited states populated by the ^{182}Pt β^+/EC decay [4]. A special question was: is the state observed at 25.7 keV an isomeric state or the first member of the rotational band built on the ground state? Moreover, the knowledge of the spin and parity values of the ^{182}Ir low-spin states was necessary to validate the proton–neutron configurations [4] proposed for some states using previous results obtained in in-beam experiments [5]. Then the comparison with the predictions of microscopic models will provide information on the proton–neutron coupling mode and on the V_{pn} interaction.

In the following, experimental procedure and results already published or presented in conferences [3,6–11], will be briefly recalled. The sharp variation observed for the M1 and E2 admixture of the $\frac{3}{2}^-\frac{1}{2}[5\,2\,1] \rightarrow \frac{1}{2}^-\frac{1}{2}[5\,2\,1]$ transitions in ^{183}Pt, ^{179,181}Os and ^{177}W will be discussed in more details.

2. Experimental procedure

Experimental setup. High-resolution measurements of low-energy conversion electrons have been performed with a magnetic spectrograph coupled to a specific tape transport system. This apparatus, presented in figure 1, was firstly installed at the on-line isotope separator ISOCELE (acceleration high voltage: 44 kV) [12]. It has been completely rebuilt to make it transportable and modified to work on-line with the ISOLDE separator (acceleration high voltage: 60 kV). The main specific elements of this apparatus are:

– A decelerating lens where the mass-separated radioactive beam is slowed from 60 kV down to 700 V and focussed in order to make a radioactive source 15 mm high and 1.5 mm wide. The deceleration of the ions before collection prevents them from being too deeply implanted; in this way, the energy lost in the collection support by the electrons emitted by the radioactive atoms is reduced and the high energy resolution is preserved for the very low-energy electrons.

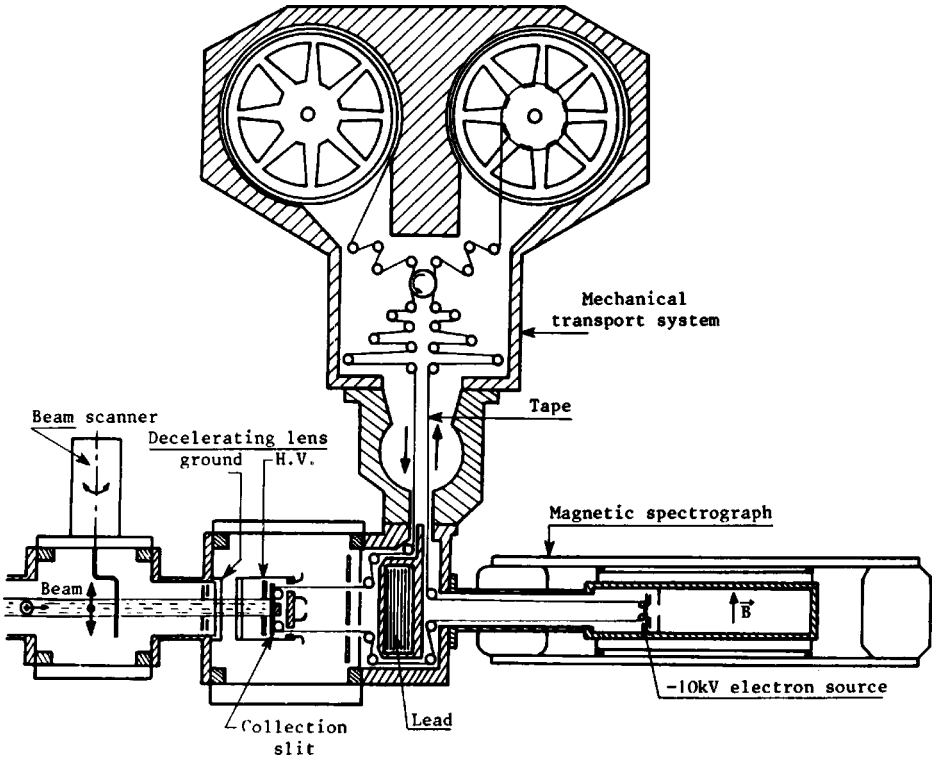

Figure 1. Front view of the experimental setup.

– A tape transport system which moves the radioactive source from the decelerating chamber to the measurement point in the magnetic spectrograph. An insulating tape on which Al deposits 15 mm long and 9 mm wide have been evaporated every 7.5 cm is used in order to apply high voltage only at the collection point (+59.3 kV) and at the electron source (~ -10 kV).
– A 180° magnetic spectrograph with an electron preacceleration system in order to overcome the energy cutoff due to the minimum radius of the spectrograph. In this way, even the very low energy electrons can reach the detector.
– A case containing the photographic film (Kodak, DEF392) used for the electron detection, equipped with two longitudinal shutters in order to determine three measurement areas on the film: upper, central and lower areas.
The magnetic induction (B) and the preacceleration high voltage (HV) applied define the energy range of the detected conversion electrons (see table 1).

Measurements and data analysis. The experiments have been performed at ISOLDE using mass-separated mercury ion beams. Mercury atoms were produced by bombarding the molten lead target [13] by the 1 GeV PS-Booster proton beam. Table 1 summarizes the experimental conditions used during the measurements. The counting

Table 1
Counting cycles, magnetic induction, preacceleration high voltage used during the experiments and energy ranges covered.

A	Decay studied	$t_{\text{collection}}$ (s)	t_{waiting} (s)	$t_{\text{measurement}}$ (s)	B (T)	HV (kV)	Energy range (keV)
187	Au → Pt	480	120	600	54×10^{-4}	0	11.0–98.3
						−10	1.0–88.3
	Au → Pt	480	120	600	60×10^{-4}	0	13.6–119.1
						−13	0.6–106.1
	Pt → Ir	1200	900	9000	60×10^{-4}	0	13.6–119.1
						−13	0.6–106.1
183	^{m}Pt → ^{g}Pt	160		160	54×10^{-4}	−10	1.0–88.3
182	Pt → Ir	270	60	330	60×10^{-4}	−13	0.6–106.1
181	^{m}Os → ^{g}Os	900		900	54×10^{-4}	0	11.0–98.3

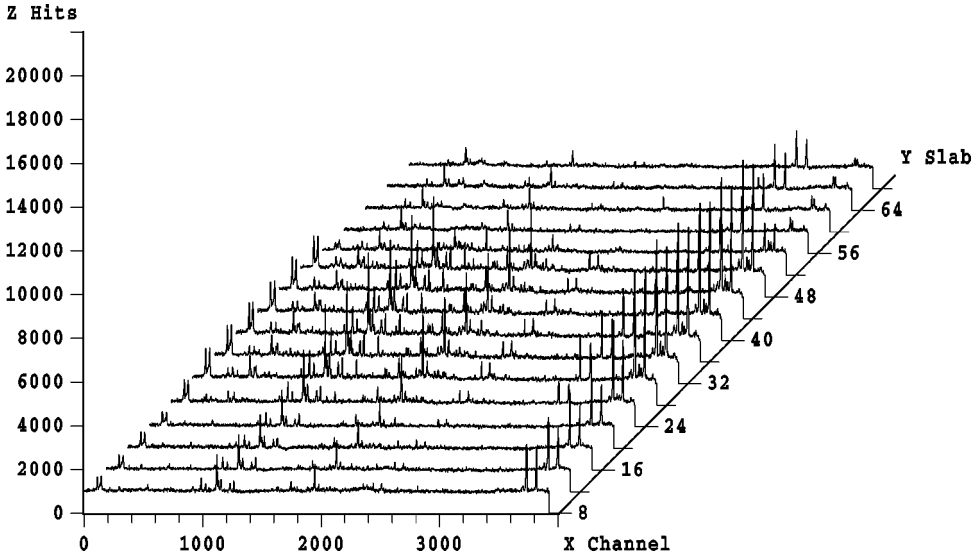

Figure 2. Three-dimensional representation of a part of the matrix corresponding to a ^{187}Au → ^{187}Pt calibration measurement. The first four spectra (lower area) correspond to the measurement with HV, the last four spectra (upper area) to the measurement without HV and the central area to the part of the film always exposed, where the electron lines obtained with and without HV are present.

cycles have been determined in order to favour the counting rate corresponding to a given decay among the radioactive chain issued from ^{A}Hg isotopes. Measurements with ^{187}Hg sources have been used for calibration because energies and intensities of the electron lines belonging to the ^{187}Au → ^{187}Pt and ^{187}Pt → ^{187}Ir decays are well known [14,15]. Moreover, two exposures, with and without the preacceleration high voltage, have been achieved on the same film in order to obtain precise values for the magnetic induction, the preacceleration high voltage and the response of the detection system (spectrograph + film). The preacceleration high voltage applied to the emitted

electrons is given in table 1. In the $A = 181$ case, a preacceleration high voltage was not really necessary since the energy of the M3 transition searched for was not very low, namely 49.0 keV [16,17].

After development, the photographic films are analysed with a microdensitometer at the CDSI Institut d'Optique (Orsay). They are scanned with a 400 μm high and 50 μm wide slit: the blackening density is digitized and stored into a bidimensional $X \times Y$ matrix where X represents, on the film, the position of the scanner in length and Y in width (see figure 2). Details about the data analysis of the electron spectra are reported in [8].

3. Experimental results

Results from the ^{183}Hg sources. Figure 3 shows a partial electron spectrum covering the electron-energy range 0–38 keV. The high energy-resolution obtained at low-energy is illustrated by the electron lines of the 16.0 keV transition in ^{183}Ir: the L_2 line, at 3.2 keV energy, is clearly observed and the doublet M_2-M_3, with a 0.36 keV energy difference, is well resolved. The total electron spectrum allowed us to determine the multipolarity of sixteen transitions (see table 2) belonging to ^{183}Pt, ^{183}Ir, ^{179}Ir, ^{179}Os or ^{179}Re, the $A = 179$ mass chain being fed by the α decay of ^{183}Hg. The 16.0 keV E2 transition in ^{183}Ir and the 35.0 keV M3 transition in ^{183}Pt are directly observed for the first time. The results concerning the M3 isomeric transition in ^{183}Pt have been presented in details elsewhere [8]. In brief, they provided the percentage branching of ^{183m}Pt by isomeric transition, $b_{IT} = 3.1 \pm 0.8\%$, and the experimental reduced transition probability, $B_{exp}(M3) = 6.8 \pm 1.8\ \mu^2 fm^4$.

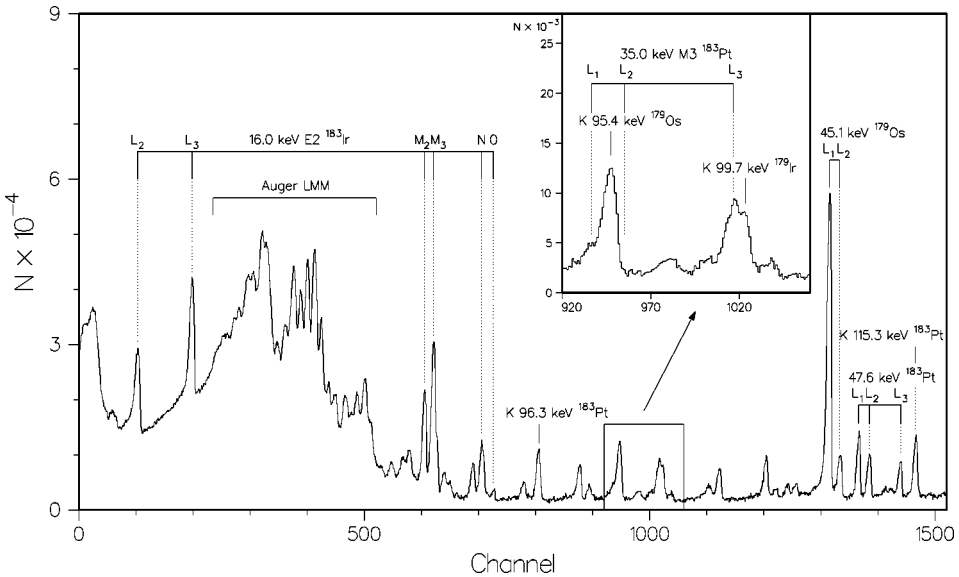

Figure 3. Partial electron spectrum obtained with ^{183}Hg sources.

Table 2
Internal electron conversion data obtained from ^{183}Hg sources.

Nucleus	E_γ (keV)	I_e[a] or α	Multipolarity
^{183}Pt	35.0	$I_{L_1} = 36 \pm 7$	M3
		$I_{L_2} < 36$	
		$I_{L_3} = 180 \pm 40$	
	47.6	$I_{L_1} = 240 \pm 50$	M1 + 7.6 ± 1.5% E2
		$I_{L_2} = 180 \pm 40$	
		$I_{L_3} = 130 \pm 30$	
	84.8	$I_{L_1} = 100 \pm 30$	E2 + 5 ± 5% M1
		$I_{L_2} = 1600 \pm 300$	
		$I_{L_3} = 1500 \pm 300$	
	96.3	$I_K = 390 \pm 80$	E2 (+M1 < 6%)
		$I_{L_3} = 900 \pm 250$	
	115.3	$\alpha_K = 0.9 \pm 0.3$	E2 (+M1 < 17%)
	124.0	$\alpha_K = 3.0 \pm 0.8$	M1 (+E2 < 30%)
^{183}Ir	16.0	$I_{L_2} = 3900 \pm 60$	E2
		$I_{L_3} = 5000 \pm 60$	
		$I_{M_1} < 77$	
		$I_{M_2} = 990 \pm 200$	
		$I_{M_3} = 1200 \pm 230$	
		$I_{N_{1+2+3}} = 510 \pm 100$	
	92.7	$\alpha_{L_1} = 1.2 \pm 0.4$	M1 (+E2 < 12%)
	118.5	$\alpha_K = 0.7 \pm 0.2$	E2 (+M1 < 10%)
^{179}Ir	93.3	$\alpha_K = 7 \pm 2$	M1 (+E2 < 20%)
	99.8	$I_{L_2} = 170 \pm 40$	E2 (+M1 < 10%)
		$I_{L_3} = 150 \pm 30$	
^{179}Os	45.1	$I_{L_1} = 1530 \pm 330$	M1
		$I_{L_2} = 190 \pm 40$	
		$I_{M_1} = 370 \pm 80$	
	86.3	$I_K = 400 \pm 100$	E2 (+M1 < 12%)
		$I_{L_3} = 770 \pm 150$	
		$I_{M_{1+2}} = 240 \pm 50$	
		$I_{M_3} = 210 \pm 50$	
	95.4	$\alpha_K \sim 6$	M1
	100.3	$I_K = 180 \pm 40$	E2 (+M1 < 10%)
		$I_{L_2} = 250 \pm 50$	
^{179}Re	53.1	$I_{L_2} = 240 \pm 50$	E2
		$I_{L_3} = 290 \pm 70$	

[a] I_{e^-} obtained with $t_{collection} = t_{measurement} = 160$ s and normalized to the total intensity (I_{total}(115.3 keV) = 1000) of the 115.3 keV ^{183}Au → ^{183}Pt transition.

Results from the ^{182}Hg sources. Table 3 gives the multipolarity determined for transitions in ^{182}Ir. In addition, a 34.0 keV E2 transition has been pointed out through its L_2, L_3, M_2 and M_3 lines in Re. We have attributed this 34.0 keV transition to

Table 3
Multipolarity of transitions in ^{182}Ir obtained from ^{182}Hg sources.

E_γ (keV)	Multipolarity	E_γ (keV)	Multipolarity	E_γ (keV)	Multipolarity
17.8	M1	57.3	E1	87.3	E2
22.0	M1	58.5	E1	95.1	M1
24.8	M1	69.3	M1 (+E2)	96.9	M1
25.7	E2	70.3	M1	101.5	M1
44.1	M1	74.7	M1 + 7.9% E2	106.8	M1
45.3	M1 + 1% E2	77.4	E1	119.5	M1
47.5	M1	81.4	E1	123.4	M1

Table 4
Internal electron conversion data obtained from ^{181}Hg sources.

Nucleus	E_γ (keV)	I_e[a] or α	Multipolarity
^{181}Os	93.8	$I_{L_1} = 120 \pm 30$	E2 (+M1 < 20%)
		$I_{L_2} = 700 \pm 150$	
		$I_{L_3} = 670 \pm 150$	
	102.7	$I_{L_1} = 60 \pm 30$	E2 (+M1 < 20%)
		$I_{L_2} = 360 \pm 80$	
		$I_{L_3} = 280 \pm 70$	
	107.6	$\alpha_K = 0.21 \pm 0.08$	E1
^{177}W	79.7	$I_{L_1+L_2} = 520 \pm 40$	E2 + 50 ± 10% M1
		$I_{L_3} = 360 \pm 80$	

[a] I_{e^-} obtained with $t_{collection} = t_{measurement} = 900$ s and normalized to the γ intensity (I_γ(107.6 keV) = 1000) of the 107.6 keV ^{181}Ir → ^{181}Os transition.

^{178}Re because the counting cycle conditions favour the counting rate associated with the ^{178}Os ($T_{1/2} = 5.0$ m) decay in comparison to that of ^{182}Os ($T_{1/2} = 22.0$ h), the $A = 178$ mass chain being fed by α decay of ^{182}Hg.

Results from the ^{181}Hg sources. Table 4 presents the transitions in ^{181}Os and ^{177}W for which the multipolarities have been determined. The K-electron lines of the 117.9 and 144.5 keV transitions in ^{181}Re have been clearly observed in the electron spectrum. As their multipolarities (M1 + E2 and E1, respectively) were already known [18], these transitions have been used in the present work to normalize both γ and electron intensities.

Concerning the search for an isomeric M3 transition in ^{181}Os, no peaks appear in the spectrum at the positions expected for the L-electron lines of a 49.0 keV transition in Os. Only upper intensity limits could be estimated for these L-electron lines and, therefore, for the percentage branching of the ^{181m}Os decay by isomeric transition: $b_{IT} \leqslant 3\%$.

4. Discussion

The multipolarities determined in the present work are in agreement with the spin and parity values previously proposed for the low-spin states in ^{183}Pt [19], ^{183,182,179}Ir [4,20–22], ^{181,179}Os [16,23], ^{179}Re [24] and ^{177}W [25]. In particular, the observation of the 16.0 keV E2 transition confirms the $\frac{9}{2}^-\frac{1}{2}$[5 4 1] and $\frac{5}{2}^-\frac{1}{2}$[5 4 1] assignments for the first excited and ground states in ^{183}Ir, respectively. In the same way, the E2 multipolarity of the 53.1 keV transition in ^{179}Re is in agreement with the configurations proposed for the levels located at 118.7 and 65.6 keV, namely, $\frac{1}{2}^-\frac{1}{2}$[5 4 1] and $\frac{5}{2}^-\frac{1}{2}$[5 4 1], respectively. The existence of the 25.7 keV E2 transition in ^{182}Ir indicates that the level located at 25.7 keV is not an isomeric state but the first rotational state built on the $\pi h_{9/2} \otimes \nu\frac{1}{2}$[5 2 1] ground state. Adding the transition multipolarities reported in table 3 to the results of an experiment under analysis, performed with a cooled Si(Li) detector coupled to a mini-orange spectrometer will allow us to assign spin and parity values to the low-spin levels in ^{182}Ir.

The results obtained on the M3 isomeric transitions in ^{183}Pt and ^{181}Os have been extensively discussed in [8]. The main conclusions of this discussion are:

- The M3 transition probabilities are very similar in ^{183}Pt and ^{184}Au. This confirms the neutron configurations proposed to describe the isomeric and ground states in ^{184}Au.
- The $\nu\frac{1}{2}$[5 2 1] $\rightarrow$ $\nu\frac{7}{2}$[5 1 4] M3 transition in the N $=$ 105 isotones does not show an obvious dependence of the Weisskopf hindrance factor (defined as $(B_{\mathrm{W}}(\mathrm{M3}))/(B_{\mathrm{exp}}(\mathrm{M3}))$, where B_{W}(M3) is the rough and simple Weisskopf estimate for a single-particle transition probability) on the quadrupole deformation, contrary to what has been observed for the other one-particle M3 transitions in the $150 < A < 190$ region.
- The determination of a precise B(M3) value in ^{181}Os, instead of a limit, is needed to study in details the evolution of the M3 hindrance factors through the N $=$ 105 isotones from ^{179}W to ^{183}Pt. With the present high-resolution energy measurement, no electron lines are seen in the energy region where the L-lines of the 49.0 keV M3 transition are expected. The analysis of new data recorded with a more efficient system including a cooled Si(Li) is still in progress and will bring new information about the M3 transition in ^{181}Os.
- The unexpected B(M3) variation for the $\nu\frac{1}{2}$[5 2 1] $\rightarrow$ $\nu\frac{7}{2}$[5 1 4] transition through the N $=$ 105 isotones is not really understood. For instance, in the frame of the Nilsson model [26] suitable to describe the odd deformed nuclei, such a variation is not reproduced: the B(M3) values calculated for ^{179}W, ^{181}Os and ^{183}Pt are quite similar and larger than the experimental ones. More sophisticated calculations are thus needed to explain the B(M3) variation through the N $=$ 105 isotones: is it due to differences in the wave functions describing the initial and final states or has the M3 effective operator to be improved?

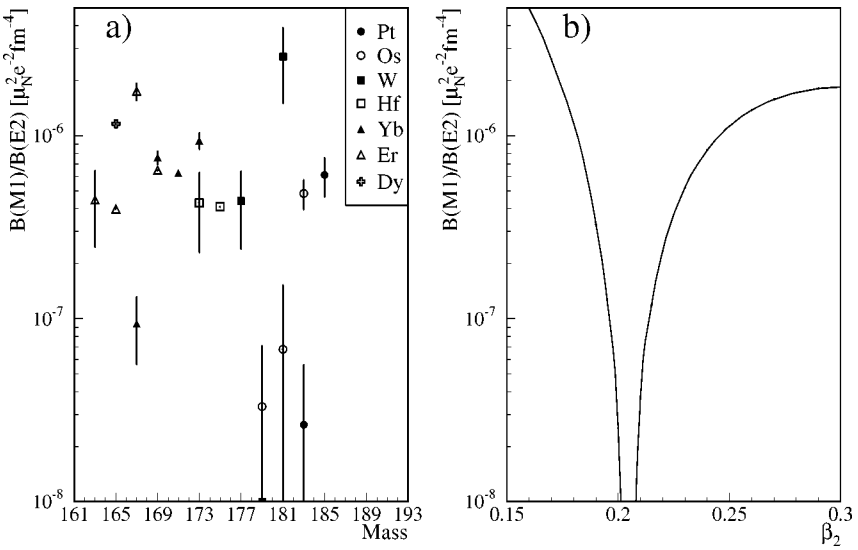

Figure 4. B(M1)/B(E2) ratios for the $\frac{3}{2}^-\frac{1}{2}$[5 2 1] $\rightarrow$ $\frac{1}{2}^-\frac{1}{2}$[5 2 1] transitions. (a) Experimental values; data are taken from this work and Nuclear Data Sheets volumes 56, 58, 62, 64, 65, 66, 68, 69, 72, 74, 75. (b) Theoretical values obtained in the Nilsson model [26] with $\kappa = 0.05$.

The following transitions: 84.8 keV in ^{183}Pt, 86.3 keV in ^{179}Os, 93.8 keV in ^{181}Os and 79.7 keV in ^{177}W are known to be the $\frac{3}{2}^- \rightarrow \frac{1}{2}^-$ transition of the $\frac{1}{2}$[5 2 1] bands. Their M1 and E2 admixtures have been determined in these experiments (see tables 2 and 4). In ^{179,181}Os and ^{183}Pt, this transition is found to be predominantly E2, whereas a mixing 50% M1 + 50% E2 has been estimated in ^{177}W. Figure 4(a) shows the ratio of the experimental reduced transition probabilities, B(M1)/B(E2), for all the known $\frac{3}{2}^-\frac{1}{2}$[5 2 1] $\rightarrow$ $\frac{1}{2}^-\frac{1}{2}$[5 2 1] transitions. Most of these transitions have a γ intensity for the M1 component higher than 50%, which corresponds to a B(M1)/B(E2) ratio lying between 4×10^{-7} and 3×10^{-6} $\mu_N^2 e^{-2} fm^{-4}$. On the contrary in ^{167}Yb, ^{179}W, ^{179,181}Os and ^{183}Pt where the transition is predominantly E2, the B(M1)/B(E2) ratios are lower than 10^{-7} $\mu_N^2 e^{-2} fm^{-4}$. It is worth noting that strong changes in the B(M1)/B(E2) ratio are observed in some isotope series, for example between ^{177,181}W and ^{179}W, between ^{183}Os and ^{179,181}Os and between ^{185}Pt and ^{183}Pt. Figure 4(b) shows the B(M1)/B(E2) ratio calculated in the frame of the Nilsson model as a function of the deformation parameter. The B(M1)/B(E2) behaviour is dominated by the changes observed in B(M1). In fact the theoretical B(E2) varies smoothly with β_2, whereas the calculated B(M1) value shows an abrupt cancellation for $\beta_2 \sim 0.2$. All this suggests deformation changes accompanied by a sharp B(M1) variation in some isotope series presented in figure 4(a). Roughly, in the $A = 160$–190 mass region, β_2 decreases when Z increases: the calculations by Möller et al. give for the ground state $\beta_2 \sim 0.29$ in ^{165}Dy, ^{165,167,169}Er and $\beta_2 \sim 0.25$ in ^{183,185}Pt [27]. For the $\frac{1}{2}$[5 2 1] states, β_2 values obtained from direct measurements like those of laser spectroscopy are available only for ^{183,185}Pt: $\beta_2(^{183g}\text{Pt}) = 0.227$ and $\beta_2(^{185m}\text{Pt}) = 0.207$ [28]. On the other hand,

microscopic calculations have been performed in the frame of the axial rotor+1 quasiparticle model [4,29] using the ^{184}Pt and ^{186}Pt cores to describe the ^{183}Pt and ^{185}Pt nuclei, respectively. An important change of the B(M1) value with the deformation is predicted too. Moreover, the B(M1) value obtained with the ^{184}Pt core constrained to the deformation determined experimentally for ^{183g}Pt is twenty times smaller than the value calculated with the ^{186}Pt core at the deformation measured experimentally for ^{185m}Pt. This seems to corroborate that the M1 and E2 admixture observed in the multipolarity of the $\frac{3}{2}^-\frac{1}{2}[5\,2\,1] \rightarrow \frac{1}{2}^-\frac{1}{2}[5\,2\,1]$ transition depends strongly on the deformation value since a small change in β_2 between two isotopes can induce an important variation in the M1 transition probability.

5. Conclusions

High-resolution measurements of low-energy conversion electrons have allowed the determination of the multipolarity of about forty low-energy transitions ($E_\gamma <$ 120 keV) in $A = 183, 182, 181, 179, 178, 177$ nuclei. The absolute intensity of the isomeric transition in ^{183}Pt has been determined; the deduced M3 transition probability is very similar to that previously obtained in ^{184}Au, which confirms the neutron configurations proposed for the ground and isomeric states in ^{184}Au. In ^{182}Ir, a 25.7 keV E2 transition has been observed, it clearly indicates that the first excited level located at 25.7 keV is not an isomeric state but the first rotational state of the $\pi h\frac{9}{2} \otimes \nu\frac{1}{2}[5\,2\,1]$ band built on the ground state. The M1 and E2 admixture has been determined for the $\frac{3}{2}^-\frac{1}{2}[5\,2\,1] \rightarrow \frac{1}{2}^-\frac{1}{2}[5\,2\,1]$ transition in ^{183}Pt, ^{181,179}Os and ^{177}W. We have shown that the sharp changes observed in the B(M1)/B(E2) ratios for this intraband transition through some isotope series can be explained by a B(M1) collapse for some deformation values. It is worth noting that the $\nu\frac{1}{2}[5\,2\,1]$ orbital plays a role in several unexpected phenomena observed in this mass region: the B(M3) behaviour in the N = 105 isotones, the B(M1)/B(E2) ratio for the $\frac{3}{2}^-\frac{1}{2}[5\,2\,1] \rightarrow \frac{1}{2}^-\frac{1}{2}[5\,2\,1]$ in ^{179}W, ^{179,181}Os and ^{183}Pt and one of the highly converted transitions observed in ^{185}Pt interpreted as the $\frac{3}{2}^-\frac{3}{2}[5\,1\,2] \rightarrow \frac{3}{2}^-\frac{1}{2}[5\,2\,1]$ transition [30].

References

[1] F. Ibrahim et al., Z. Phys. A 350 (1994) 9.
[2] F. Ibrahim et al., Phys. Rev. C 53 (1996) 1547.
[3] B. Roussière et al., in: *Proc. of the 8th Internat. Symp. on Capture Gamma-Ray Spectroscopy and Related Topics*, ed. J. Kern (World Scientific, Singapore, 1994) p. 231.
[4] J. Sauvage et al., Nuclear Phys. A 592 (1995) 221.
[5] A.J. Kreiner et al., Phys. Rev. C 42 (1990) 878.
[6] B. Roussière et al., in: *Proc. of the Internat. Conf. on the Future of Nuclear Spectroscopy*, eds. W. Gelletly, C.A. Kalfas, S. Harissopulos and D. Loukas (I.N.P., NCSR Demokritos, 1994) p. 17.
[7] B. Roussière et al., in: *Proc. of the Internat. Conf. on Exotic Nuclei and Atomic Masses, ENAM '95*, eds. M. de Saint-Simon and O. Sorlin (Editions Frontières, 1995) p. 593.

[8] B. Roussière et al., Nuclear Phys. A 643 (1998) 331.
[9] J. Sauvage et al., in: *Proc. of the Internat. Conf. on Exotic Nuclei and Atomic Masses, ENAM '95*, eds. M. de Saint-Simon and O. Sorlin (Editions Frontières, 1995) p. 597.
[10] J. Sauvage et al., in: *Proc. of the Internat. Workshop on Hyperfine Structure and Nuclear Moments of Exotic Nuclei by Laser Spectroscopy*, JINR E15-98-57 (1998) p. 108.
[11] J. Sauvage et al., in: *Internat. Conf. on Nuclear Physics Close to the Barrier*, Warsaw, Poland (1998).
[12] P. Kilcher et al., Nucl. Instrum. Methods A 279 (1989) 485.
[13] J. Lettry et al., in: *ICANS XIII, Joint Proc. of the 13th Meeting of the Internat. Collaboration on Advanced Neutron Sources*, PSI-Proc. 95-02 (Villigen, Switzerland, 1995) p. 595.
[14] A. Ben Braham et al., Nuclear Phys. A 332 (1979) 397.
[15] C. Sébille-Schück et al., Nuclear Phys. A 212 (1973) 45.
[16] B. Roussière et al., Z. Phys. A 351 (1995) 127.
[17] T. Kutsarova et al., Nuclear Phys. A 587 (1995) 111.
[18] C.M. Lederer and V.M. Shirley, *Table of Isotopes*, 7th ed. (Wiley, New York, 1978).
[19] B. Roussière et al., Nuclear Phys. A 504 (1989) 511.
[20] A. Visvanathan et al., Phys. Rev. C 19 (1979) 282.
[21] A. Zerrouki, Thèse 3ème cycle, Université Paris-Sud (1979).
[22] F. Meissner et al., Phys. Rev. C 48 (1993) 2089.
[23] U. Bosch et al., Z. Phys. A 341 (1992) 245.
[24] C. Baglin, Nucl. Data Sheets 72 (1994) 617.
[25] E. Browne, Nucl. Data Sheets 68 (1993) 747.
[26] S.G. Nilsson, Dan. Mat. Fys. Medd. 29 (1955) 16.
[27] P. Möller et al., Atom. Data Nucl. Data Tables 59 (1995) 185.
[28] F. Le Blanc et al., in: *Proc. of Internat. Conf. on Exotic Nuclei and Atomic Masses, ENAM '98*, Bellaire (1998), eds. B.M. Sherrill, D.J. Morrissey and C.N. Davids, AIP Conf. Proc. 455 (1998) p. 78.
[29] M. Meyer et al., Nuclear Phys. A 316 (1979) 93.
[30] B. Roussière et al., Nuclear Phys. A 485 (1988) 111.